

Mountaintop and radar measurements of anthropogenic aerosol effects on snow growth and snowfall rate

Randolph D. Borys and Douglas H. Lowenthal

Storm Peak Laboratory, Division of Atmospheric Sciences, Desert Research Institute, Reno, NV, USA

Stephen A. Cohn and William O. J. Brown

National Center for Atmospheric Research, Atmospheric Technology Division, Boulder, CO, USA

Received 30 December 2002; revised 20 February 2003; accepted 11 March 2003; published 30 May 2003.

[1] A field campaign designed to investigate the second indirect aerosol effect (reduction of precipitation by anthropogenic aerosols which produce more numerous and smaller cloud droplets) was conducted during winter in the northern Rocky Mountains of Colorado. Combining remote sensing and in-situ mountain-top measurements it was possible to show higher concentrations of anthropogenic aerosols ($\sim 1 \mu\text{g m}^{-3}$) altered the microphysics of the lower orographic feeder cloud to the extent that the snow particle rime growth process was inhibited, or completely shut off, resulting in lower snow water equivalent precipitation rates. **INDEX TERMS:** 0305 Atmospheric Composition and Structure: Aerosols and particles (0345, 4801); 0320 Atmospheric Composition and Structure: Cloud physics and chemistry; 0345 Atmospheric Composition and Structure: Pollution—urban and regional (0305); 1610 Global Change: Atmosphere (0315, 0325); 1655 Global Change: Water cycles (1836). **Citation:** Borys, R. D., D. H. Lowenthal, S. A. Cohn, and W. O. J. Brown, Mountaintop and radar measurements of anthropogenic aerosol effects on snow growth and snowfall rate, *Geophys. Res. Lett.*, 30(10), 1538, doi:10.1029/2002GL016855, 2003.

1. Introduction

[2] Mountaintop and remotely sensed data on aerosols and cloud and precipitation microphysics and chemistry were collected in wintertime synoptic scale storm systems to investigate the second indirect aerosol effect on precipitation formation. When storm systems encounter mountains or plateaus, additional lifting at low levels is produced, enhancing the larger scale lifting and resulting in production of additional condensate available for scavenging by precipitation formed at higher levels. This mechanism has been referred to as a “seeder-feeder” couplet by *Reinking et al.* [2000] which enhances precipitation in higher terrain. The second indirect aerosol effect arises due to elevated concentrations of cloud condensation nuclei (CCN), typically man-made, which results in clouds with higher droplet concentrations and smaller mean diameters and may reduce precipitation formation. In a mixed-phase cloud the smaller mean droplet size can significantly reduce ice particle rime growth efficiencies [*Pruppacher and Klett*, 1980]. Our working hypothesis is that less accumulated snowfall water equivalent (SWE) will precipitate to the surface due to the reduction of ice particle growth by rime when anthropogenic aerosol is present.

[3] Measurements were made at Storm Peak Laboratory (SPL, <http://stormpeak.dri.edu>) at the summit of Mt. Werner (3210m AMSL) 9 km east of Steamboat Springs, CO and from a National Center for Atmospheric Research (NCAR, <http://www.atd.ucar.edu>) Integrated Sounding System (ISS, *Parsons et al.*, 1994, in the valley 6.5 km upwind at 2067m AMSL). The ISS consisted of a GPS/LORAN Atmospheric Sounding System (GLASS) and a Multiple Antenna Profiler Radar (MAPR, *Cohn et al.*, 2001). (<http://www.atd.ucar.edu>). The simultaneous mountaintop and valley measurements allowed characterization of the cloud and snowfall in-situ while the remote sensing radar monitored the wind velocity, snow origin height and snow fall-speed upwind. The valley site had a complete surface meteorological station including two SWE snow gages and was 10 minutes upwind in a typical 10 m/s wind speed at the elevation of SPL. Unlike Doppler beam swinging wind profilers, MAPR measures the vector wind using spaced antenna methods and a continuously vertically directed beam. The radar can measure the snow vertical fall-speed with very good time resolution.

[4] We present measurements from two days which support the working hypothesis and demonstrate the coherence among the data sets and instrumentation. February 15 and February 19, 2001 were two snowfall events which had contrasting snow growth processes. Feb. 15 is a case where clouds were shallow and growth was primarily by diffusion. On Feb. 19 the clouds were deeper and the growth was primarily by rime. In both cases the lower orographic feeder cloud had the same supercooled cloud liquid water (SCLW, g m^{-3}) content measured at SPL but dramatically different droplet size distributions. This difference will be shown to cause the different snow growth and snowfall rates.

2. Valley and Remote Sensor Observations

[5] Figure 1 shows time-height plots of the MAPR signal to noise ratio, vertical velocity, and horizontal wind velocity on February 15 and 19. On Feb. 15 in-situ measurements were taken at SPL between 1545 and 1630 UTC. During this period, the top of the backscatter layer (cloud top) was about 2 km above the radar site with a cloud top temperature of -19°C and typical snow fall-speeds of 1.0 m s^{-1} . On Feb. 19 in-situ measurements were taken at SPL from 1525 to 2100 UTC. MAPR backscatter extended to 3.5 km AGL with snow fall-speeds consistently increasing with decreasing altitude indicating continued snow growth by accretion of SCLW in the orographic feeder cloud. Fall-speeds were generally 1.5 m s^{-1} in the feeder cloud. A rawinsonde

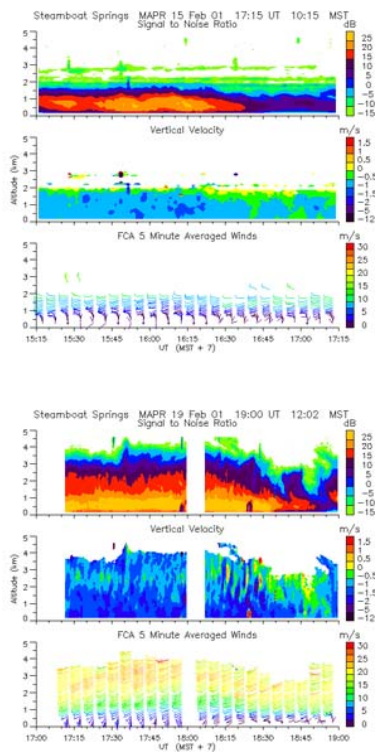


Figure 1. Time-height plots from MAPR for Feb. 15 and 19, 2001.

launched at 1823 UTC on February 19 showed a cloud top temperature of -22°C at 3.5 km AGL, consistent to where MAPR showed the first backscatter from snow.

[6] The ISS recorded surface snowfall with a weighing bucket gage as SWE. Figure 2 shows the snowfall time series on Feb. 15 and 19. No snow was recorded at the ISS during the period of measurement at SPL (1545–1630 UTC) even if a 20 minute upwind drift time is included. On Feb. 19 the snow gage measured SWE of about 0.7 mm hr^{-1} during the period of measurement at SPL (1525 to 21005 UTC). Wind speed, direction, temperature and relative humidity were all similar on both days.

[7] Figure 3 shows Mosimann’s riming index (R_m , Mosimann, 1995) derived from the ISS snow fall-speed

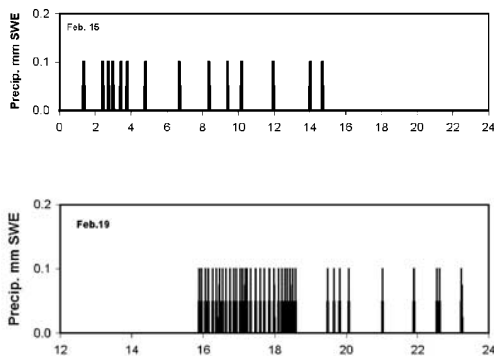


Figure 2. Precipitation time series at the ISS for Feb. 15 (top) and Feb. 19 (bottom). Time UTC.

and snow particle habit from SPL observations. For this measurement we adjusted the equation of Mosimann for air density and assumed that the vertical air motion at the radar position upwind of the mountain included both positive and negative values which would not be biased in either direction. This index ranges from 0–5, with 0–3 indicating snow particles which respectively are unrimed, 25, 50, and 100% rimed. An index of 4 or 5 indicates crystals with several layers of rime ice or graupel. Figure 3 shows that at the elevation of SPL, the index was 0–1 for the observation period on Feb. 15 and 0–3 on Feb. 19.

3. In-Situ Measurements at Storm Peak Laboratory

[8] Measurements at SPL were done during sampling periods. The sample period on Feb. 15 was from 1545–1630 UTC and the period on Feb. 19 was from 1815–1845 UTC. The period on Feb. 19 is representative of six sampling periods on that day. A sample period consisted of simultaneous integrated cloud droplet and snow size spectra, a video record of the snow crystal habit and riming extent, snowfall rate measurements and snow and cloud water collections. The snow and cloud water were analyzed for ionic and oxygen isotopic content. Cloud droplet and snow size spectra from DMT SPP-100 and 2DP particle probes were integrated over the entire sampling period on each day. Results are plotted in Figure 4.

[9] Video images of snow crystals are shown in Figure 5. The transparent appearance of the images on Feb. 15 indi-

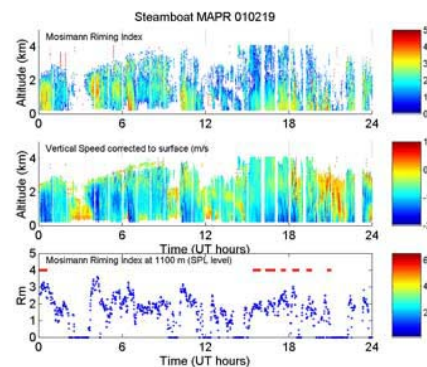
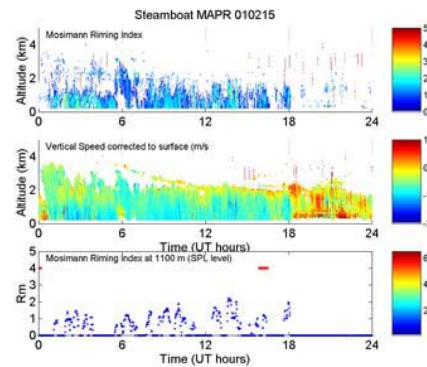


Figure 3. MAPR derived vertical time series cross-section of riming index at SPL elevation for Feb. 15 and 19, 2001.

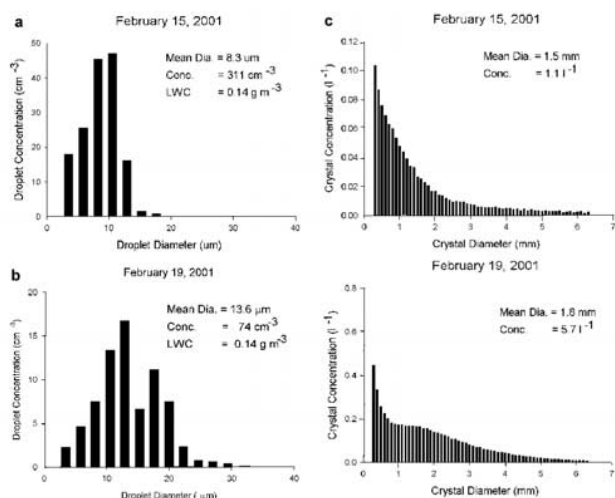


Figure 4. Cloud droplet and snow size spectra for the sampling periods on Feb. 15 and 19, 2001.

cates there are no rime ice deposits on the crystals. The habits are dominated by dendrites. On Feb. 19 crystals are opaque, indicating moderate to heavy rime ice deposits. The degree of rime was confirmed by visual observation of snow crystals under high magnification. Habits on this day included sector plates, broken dendritic branches, and some needles. The droplet measurements support the rime observations.

[10] On Feb. 15, the unrimed case day, the cloud droplet number mean diameter was $8.3 \mu\text{m}$, the concentration was 310 cm^{-3} and the SCLW content was 0.13 g m^{-3} . In contrast, the droplet spectra on Feb. 19, the rimed case day, had a number mean diameter of $13.6 \mu\text{m}$, a concentration of 74 cm^{-3} , and a SCLW content of 0.14 g m^{-3} . More than 80% of the droplet number and 98% of the SCLW in the rimed case was in droplets greater than $10 \mu\text{m}$ dia. In contrast, most of the droplets and the SCLW in the unrimed case were in diameters well below this size.

[11] The snow size spectra for the two cases showed more subtle differences (Figure 4). The mean diameters differed by 0.3 mm with the rimed case being larger. The rimed case had a five-fold higher snow particle number concentration. Snowfall rates measured at SPL during the sample periods

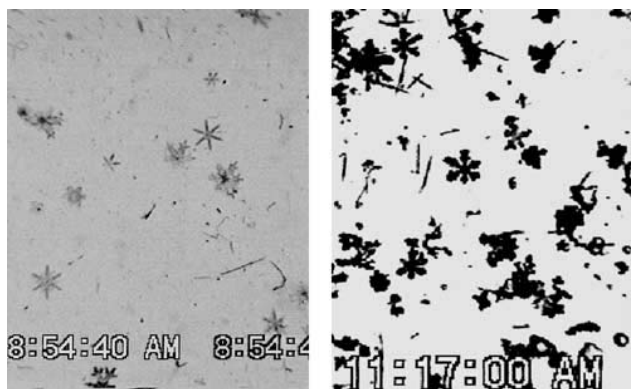


Figure 5. Video images of snow particles on Feb. 15 (left) and Feb. 19 (right).

Table 1. Chemical and Physical Properties of Cloud Droplets and Snow During Two Precipitation Events

February	15	19
Major Habit	Planar Dendrite	Planar Dendrite
Rime Category	Unrimed (0.5)	Moderate (2.0)
Rime Mass Frac.	5%	51%
SPL Precip. Rate	0.02 mm hr^{-1}	0.38 mm hr^{-1}
ISS Precip. Rate	0 to 0.1 mm hr^{-1}	1.1 mm hr^{-1}
SPL Temperature	-13°C	-4°C
Snow $\delta^{18}\text{O}$	-22.1	-16.5
Cloud $\delta^{18}\text{O}$	-21.1	-16.2
$\delta^{18}\text{O}$ Snow Mass	-14°C	-4.8°C
Temp. Of Origin		
Cloud Top Temp	-19°C	-22°C
Snow CAE SO_4^-	$0.011 \mu\text{g m}^{-3}$	$0.072 \mu\text{g m}^{-3}$
Cloud CAE SO_4^-	$1.1 \mu\text{g m}^{-3}$	$0.12 \mu\text{g m}^{-3}$
Droplet Mean Dia.	8.3 mm	13.6 mm
Droplet Conc.	310 cm^{-3}	74 cm^{-3}
Cloud SCLW	0.13 g m^{-3}	0.14 g m^{-3}

on Feb. 15 and 19 were 0.02 mm hr^{-1} and 0.38 mm hr^{-1} , respectively.

4. Discussion

[12] The valley and mountain-top measurements and observations showed that precipitation rates were higher when snow growth included riming. Also, whether riming occurred was clearly due to the presence or absence of large ($>10 \mu\text{m}$ dia.) cloud droplets. Now, to test our working hypothesis we need to 1) show that anthropogenic aerosol was responsible for the change in cloud droplet size and 2) prove that the difference in precipitation rates was due to the relative importance of snow growth by accretion of cloud droplets. To facilitate this discussion, Table 1 summarizes the data for both days.

[13] The smaller mean droplet diameter on Feb. 15 may be related either to the level of cloud base below SPL or to the CCN concentration that produced the cloud. Cloud base height was not measured. However, SCLW and the valley temperature and relative humidity values were essentially the same in each case suggesting cloud base heights were similar. Further, previous work has shown the clear-air-equivalent (CAE) concentration of anthropogenic sulfate in the atmosphere (the product of the SCLW content, g m^{-3} , and the cloud water anthropogenic sulfate concentration, $\mu\text{g g}^{-1}$) is negatively correlated with the cloud droplet size and positively correlated with the number concentration at SPL [Borys *et al.*, 2000]. CAE anthropogenic sulfate is used here as an indicator of a polluted air mass. There are likely other species involved as well. However, anthropogenic sulfate is a major component of the total ionic species present and covaries with other pollutants in general [Borys *et al.*, 2000]. Determining CAE concentrations from cloud water, we suggest, is a surrogate method of measuring the composition of CCN.

[14] The CAE anthropogenic sulfate concentration for the unrimed case on Feb. 15 ($1.07 \mu\text{g m}^{-3}$) was 8.9 times higher than that found in the rimed case ($0.12 \mu\text{g m}^{-3}$) on Feb. 19. Thus, there were more anthropogenic CCN present on Feb. 15 than on Feb. 19.

[15] The ISS SWE precipitation rate was 0.7 mm hr^{-1} on Feb 19 and $0 - 0.1 \text{ mm hr}^{-1}$ on Feb. 15. At SPL, the snowfall rate was 19-times higher on Feb. 19 than on the

15th. The snow particle number concentration was 5-times higher and mean diameter was 0.3 mm larger on Feb. 19. The combination of the number, concentration, mean diameter and dominant snow particle habit (dendrite) mass-dimensional size relationship produces a seven-fold higher precipitation rate on the rimed case day, the minimum difference observed. The larger mean snow particle size fall speed would be 4 cm s^{-1} (8%) greater, insufficient to enhance riming efficiencies or precipitation rates by the amount observed. The rimed-mass-fraction also may contribute significantly to the snowfall rate. The visual and video observations of rimed crystals and higher fallspeeds indicated by the MAPR suggest that the higher snowfall rate on the Feb. 19 was due in part to snow growth by riming.

[16] The rimed mass fraction of the snow crystals can be quantitatively determined using the method of *Puxbaum and Tschewenka* [1998] if we assume that fine-particle sulfate aerosols primarily served as CCN and that the cloud droplets measured and collected at SPL are representative of the droplets collected by the snow particles. Using this method and the sulfate ion concentrations in snow and cloud water, 4.5% and 51% of the snow mass was attributable to riming on Feb. 15 and Feb. 19, respectively. Thus one half of the higher snowfall rate on Feb. 19 resulted from snow growth by riming. The remainder resulted from growth by diffusion. The higher snow particle concentration on Feb. 19 enhanced the role of riming by having more numerous cloud droplet collectors.

[17] To determine the mass-weighted elevation of the growth of the rimed snow we utilized a temperature of formation estimate based on the oxygen isotopic composition of the cloud and snow water expressed as a deviation from Vienna Standard Mean Ocean Water (V-SMOW), $\delta^{18}\text{O}$. In a rising parcel of cloudy air, this value becomes more negative as the temperature decreases. As shown by *Warburton and DeFelice* [1986] the relationship with temperature in Sierra Nevada storms is $\delta^{18}\text{O} = 0.9T - 3.4$, where T is $^{\circ}\text{C}$. *Picciozzo et al.* [1960] found a similar relationship, $\delta^{18}\text{O} = 0.9T - 6.4$, in Antarctic storms. The slope is the same in both cases. The $\delta^{18}\text{O}$ of the cloud water at SPL provides a reference for riming occurring at the elevation of SPL. The expected change in $\delta^{18}\text{O}$ with height above SPL can be predicted using the value measured at SPL and the temperature lapse rate. Small differences in $\delta^{18}\text{O}$ between ice phase deposition and water phase condensation can be ignored. Freezing SCLW preserves the $\delta^{18}\text{O}$ of the original water.

[18] A measure of the difference between $\delta^{18}\text{O}$ of cloud water, which has no appreciable fallspeed and anchors the $\delta^{18}\text{O}$ to the air temperature at SPL, and snow water, which does have an appreciable fallspeed, will give a temperature of the elevation where the majority of the snow water formed. The data are presented in Table 1. On each day the difference between the $\delta^{18}\text{O}$ of the snow and cloud water was small but between days the absolute values were quite different. This indicates snow mass growth occurred at or near the elevation of SPL on each day even though cloud top temperatures were 6°C and 18°C colder than the air temperature at SPL on Feb. 15 and 19, respectively.

[19] The unrimed snow $\delta^{18}\text{O}$ differs little from the cloud water because snow particle trajectories can be very horizontal, especially for small, planar crystals (*R. Rauber, Colorado State University, M.S. Thesis, 1986*). The rimed

snow which has higher fall speeds and larger sizes may have originated near cloud top several km above SPL but clearly obtained most of its mass near the elevation of SPL as accreted cloud water. Given that the cloud on both days had the same SCLW the effect of anthropogenic aerosol on Feb. 19 was to effectively eliminate additional potential snow growth by riming.

[20] The difference between the cloud CAE anthropogenic aerosol sulfate concentrations on the two days is nearly an order of magnitude, but in absolute terms it is only $1 \mu\text{g m}^{-3}$. Astonishingly, this small amount of aerosol can reduce the snowfall rate up to 50%.

5. Conclusions

[21] Evidence is presented to demonstrate the possible magnitude of the secondary indirect aerosol effect on precipitation rates from cold, mixed-phase clouds in mountainous regions where a seeder-feeder cloud couplet is present. Changes as small as $1 \mu\text{g m}^{-3}$ in CCN aerosol concentration can cause significant changes in cloud properties and precipitation efficiencies.

[22] **Acknowledgments.** This work was supported by the National Science Foundation Division of Atmospheric Sciences grant ATM-0004265. Logistical assistance from the Steamboat Ski and Resort Corporation is greatly appreciated. Special thanks to the support personnel from NCAR-ATD who were responsible for the installation setup and operation of the ISS and ancillary equipment including Ned Chamberlain, Mike Susedik, and Terry Hock. We also appreciate the instrument development work done by Rick Purcell and Dan Wermers at DRI. DRI is an equal opportunity service provider and employer and is a permittee of the Medicine-Bow and Routt National Forests.

References

- Borys, R. D., D. H. Lowenthal, and D. L. Mitchell, The relationships among cloud microphysics, chemistry, and precipitation rate in cold mountain clouds, *Atmospheric Environment*, 34, 2593–2602, 2000.
- Cohn, S. A., W. O. J. Brown, C. L. Martin, M. S. Susedik, G. Maclean, and D. B. Parsons, Clear air boundary layer spaced antenna measurements with the Multiple Antenna Profiler (MAPR), *Annals Geophysicae*, 19, 845–854, 2001.
- Mosimann, L., An improved method for determining the degree of snow crystal riming by vertical Doppler radar, *Atmospheric Research*, 37, 305–323, 1995.
- Parsons, D. B., W. Dabberdt, H. Cole, T. Hock, C. Martin, A. L. Barrett, E. Miller, M. Spowart, M. Howard, W. Ecklund, D. Carter, K. Gage, and J. Wilson, The Integrated Sounding System: Description and Preliminary Observations from TOGA COARE, *Bulletin of the American Meteorological Society*, 75(4), 553–568, 1994.
- Puxbaum, H., and W. Tschewenka, Relationships of major ions in snow fall and rime at Sonnblick Observatory (SBO, 3106 m) and implications for scavenging processes in mixed clouds, *Atmos. Environ.*, 32, 4011–4020, 1998.
- Picciozzo, E., X. DeMaere, and L. Friedman, Isotopic composition and temperature of formation of antarctic snows, *Nature*, 187, 857–859, 1960.
- Pruppacher, H. R., and J. D. Klett, *Microphysics of Clouds and Precipitation*. D. Reidel Publishing Co., 714 pp., 1980.
- Reinking, R. F., J. B. Snider, and J. L. Coen, Influences of storm-embedded orographic gravity waves on cloud liquid water and precipitation, *Journal of Applied Meteorology*, 39, 733–759, 2000.
- Warburton, J. A., and T. P. DeFelice, Oxygen isotopic composition of central Sierra Nevada precipitation. I: Identification of ice-phase water capture regions in winter storms, *Atmospheric Research*, 20, 11–22, 1986.

R. D. Borys and D. H. Lowenthal, Storm Peak Laboratory, Division of Atmospheric Sciences, Desert Research Institute, Reno, NV, USA 89512-1095. (borys@dri.edu)

S. A. Cohn and W. O. J. Brown, National Center for Atmospheric Research, Atmospheric Technology Division, Boulder, CO, USA 80307-3000.